Active Control of Compressor Instability and Surge by Stator Blades Adjustment

M. T. Schobeiri* and M. Attia†
Texas A&M University,
College Station, Texas 77843-3123

Introduction

THE inception of compressor instability in general occurs during an adverse operation condition that may cause an increase in compressor blade incidence angle and, thus, higher flow deflection. Reducing the compressor mass flow at a given rotational speed past the design surge limit exhibits one of the typical scenarios that can force the compressor into unstable operation. The decreased axial velocity component caused by the mass flow reduction changes the incidence angle leading to an increased flow deflection that results in a pressure increase. The increased pressure, however, may cause the velocity profile within the boundary layer to approach its separation point. In this case, the fluid particle inside the blade surface boundary layer is, roughly speaking, exposed to three different forces. The convective force tries to move the particle in the direction of the motion, whereas two coacting forces, the shear stress force and the pressure force, oppose the motion of the particle. These three forces are generally in a dynamic equilibrium condition, which can be disrupted if additional pressure buildup is triggered by an adverse off-design operating point that leads to increased flow deflection. This situation leads to a major boundary-layer flow separation along the blade surface, hub, and casing, which indicates the inception of compressor instability. The phenomenon of the flow separation (stall) and its control has been well known in external aerodynamics for more than half a century, where Prandtl, Schlichting,[1] and Betz[2] suggested several different control scenarios. Stability enhancement using casing treatment was suggested by several researchers and summarized by Greitzer.[3]

The method discussed in this Note deals with the aerodynamic control and prevention of axial compressor instability and surge. It is based on dynamically adjusting the stator blades to the compressor interstage unsteady aerodynamics. Although it is concentrated on the aerodynamic control and prevention of stall, the method does not deal with control specific procedures and algorithms. However, it can be combined with any multivariable control system to provide an active feedback control to prevent inception of compressor instability during a dynamic operation.

Active Instability and Surge Prevention by Adjusting the Stator Blades

The instability and surge prevention and aerodynamic control discussed is applied to high-performance gas turbine engines with adjustable compressor stator blade rows. It is probably the most effective active aerodynamic control mechanism. In contrast to the active control procedures found in the open literature, this type of control procedure is held proprietary by the engine manufacturer, and, consequently, there is little information available. Figure 1 shows schematically the configuration of a multistage compressor with adjustable stator blade rows. Figure 1a shows the stator blade adjustment by changing the stagger angle γ. Figures 1b and 1c show schematically the effect of blade adjustment on the stage velocity diagram. Figure 1b shows the stator row in its design stagger position under the adverse operation condition that is associated with an increase in compressor pressure ratio. This pressure ratio, however, is established by a deflection angle ϑ that may cause a boundary-layer separation on stator and rotor blades, thus, leading to an inception of rotating stall and surge condition. To prevent this, the stagger angle γ is adjusted, which results in a reduced ϑ. The flow deflection along the stator or rotor cascade with the velocity diagram is shown in Fig. 1c. It is directly related to specific circulation functions, which is a crucial part of the diffusion factor of the corresponding blade row. We use the ratios

$$\phi = V_{a2}/U_2, \qquad \nu = U_1/U_2 = r_1/r_2$$
$$u = V_{a1}/V_{a2} = W_{a1}/W_{a2}, \qquad C_\Gamma = A/\rho_\infty V_\infty V_{a1} s$$

with the axial components V_a, W_a of the velocity vectors defined in Fig. 1b, where C_Γ is the circulation function and A is the lift force. For the stator row, we obtain the modified diffusion factor,[4]

$$D'_m = 1 - \frac{1}{\mu}\frac{\sin\alpha_1}{\sin\alpha_2} + \frac{\nu \sin^2\alpha_1}{\sigma(\nu+1)}\left[\cot\beta_1 - \frac{1}{\mu\nu}\cot\alpha_2\right] \times \left[1 - M_1^2\left(\frac{1}{\mu}\frac{\sin\alpha_1}{\sin\alpha_2}\right)\left(\frac{1}{\mu}\frac{\sin\alpha_1}{\sin\alpha_2} - 1\right)\right] \tag{1}$$

and for the rotor row, we have the diffusion factor

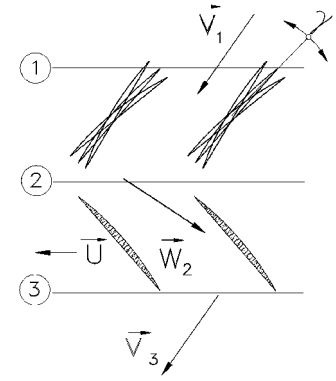

Fig. 1a Compressor stage with adjustable stator rows.

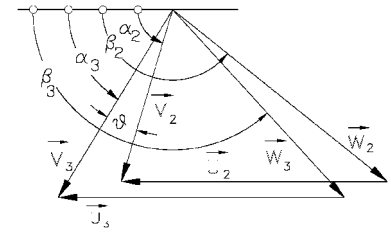

Fig. 1b Velocity diagram.

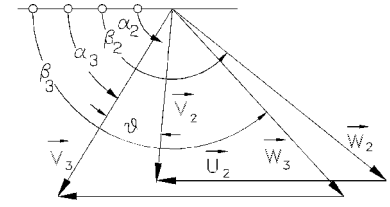

Fig. 1c Adjusted stator, increased deflection.

Received 3 August 2001; revision received 7 December 2002; accepted for publication 20 December 2002.

*Professor of Mechanical Engineering, Turbomachinery Performance and Flow Research Laboratory, Department of Mechanical Engineering. Member AIAA.

†Research Assistant, Turbomachinery Performance and Flow Research Laboratory, Department of Mechanical Engineering.

$$D''_m = 1 - \frac{1}{\mu}\frac{\sin\beta_2}{\sin\beta_3} + \frac{\nu\sin^2\beta_2}{\sigma(\nu+1)} \times \left[\frac{-1}{\mu\nu\phi}(1-\nu^2) + \cot\beta_2 - \frac{1}{\mu\nu}\cot\beta_3\right] \times \left[1 - M_2^2\left(\frac{1}{\mu}\frac{\sin\beta_2}{\sin\beta_3}\right)\left(\frac{1}{\mu}\frac{\sin\beta_2}{\sin\beta_3} - 1\right)\right] \quad (2)$$

with α_1, α_2, β_2, and β_3 as the inlet and exit flow angle of the corresponding stator and rotor row, respectively. The first left brackets on the left-hand side in Eqs. (1) and (2) represent the circulation function, whereas the right brackets account for compressibility effects. Adjusting the stator blades will reduce the deflection on both stator and rotor blades, which results in a decrease of the diffusion factor and, thus, prevents the compressor blade boundary-layer flow from separation that would trigger the inception of rotating stall and surge. In contrast to the methods found in the literature, the instability and surge prevention presented here, does not use maps. However, it requires knowledge of the blade inlet and exit camber angles, as well as its loss behavior with respect to changes of the diffusion factor. With this information, the compressor design and off-design behavior can be determined using either a stage-by-stage or a row-by-row calculation procedure. A row-by-row calculation procedure was found to be more accurate and computationally stable. The procedure is then implemented into GETRAN for a full dynamic calculation.

Row-by-Row Compressor Calculation

The row-by-row flow analysis method used is based on a one-dimensional calculation of the compression process using a set of dimensionless row parameters. These parameters, along with the loss correlations developed by Schobeiri,[4,5] describe the design and off-design behavior of the compressor. For the present investigations, the loss calculation procedure[4] was used that correlates the individual losses such as the profile, secondary, and shock losses with the modified diffusion factor by Eqs. (1) and (2). As shown in Fig. 2, a set of curves representing the blade total loss parameter $\zeta_t \sin(\alpha_{in}, \beta_{in})/2\sigma$ is plotted, with α_{in} and β_{in} as the inlet flow angles of stator or rotor row and σ as the cascade solidity. For a one-dimensional application, the loss distribution must be integrated over the blade height by applying the energy balance to the individual mass flows through the stream tubes shown in Fig. 2.

By use of the described method, the performance behavior of the compressor under any adverse operation condition can be calculated. Note that the method does not use steady-state maps; however, it easily can generate one. This is demonstrated by reproducing the performance maps for the compressor of a GT-9 gas turbine engine, whose detailed data were published by Attia and Schobeiri.[6] The compressor of this gas turbine has three performance maps. The first map covers the performance ranges of the three front stages, which we refer to as the low-pressure (LP) stages. The second map covers the three intermediate pressure (IP) stages, and the third map covers the performance range of the remaining nine stages, which we refer to as the high-pressure (HP) stage group. The purpose of this stage decomposition was to make sure that the present method is capable of accurately reproducing the known compressor stage maps before implementing the method into the dynamic code GETRAN.

Because the diffusion factor is calculated automatically during an off-design operation, it is convenient to construct the surge limits by introducing a stall diffusion factor. When the maximum incidence range discussed earlier is considered, the stall diffusion factors of $D_m = 0.5$–0.6 were chosen for all reduced rotational speeds. As an example, Fig. 3 shows the performance map of the LP stage groups of the power generation gas turbine engine GT-9 discussed subsequently. Figure 3 shows the row-by-row calculated pressure ratio Π as a function of reduced volume ratio (VR) with reduced rotational speed as a parameter. To verify the calculation results, the actual pressure curves for different reduced rotational speeds are also plotted in Fig. 3 ($\triangle$). Comparison with the actual data indicates that the method accurately predicts the compressor off-design performance and can be implemented into the dynamic code GETRAN with confidence. The effect of the stator blade adjustment on the compressor performance and stability is demonstrated by varying the stagger angle for the IP part (Fig. 4). When a start from a constant design speed and the design stagger angle of $\gamma_0 = 51.8$ deg is considered, it is varied from $\gamma = 15$ to 65 deg. As can be seen, decreasing the stagger angle below the design point allows a significant reduction of the volume flow, which would not have been possible at the design stagger angle. The volume flow can be reduced to less than 40% without encountering instability. On the other hand, increasing γ shifts the surge limit substantially above the design point, thus, preventing the compressor from entering into an unstable operating regime.

Integration of the Procedure into GETRAN

To predict the dynamic response of compressors to adverse operation conditions, a compressor module with adjustable stator blade row, discussed earlier, was developed and integrated into the dynamic simulation code GETRAN[7] as an autonomous module. GETRAN is a generic, modularly structured computer code for simulation of transient behavior of aero- and power-generation gas turbine engines. The code is capable of simulating the nonlinear dynamic behavior of single- and multispool core engines, turbofan engines, and power-generation gas turbine engines and their individual components under adverse dynamic operating conditions. The individual components, as well as their couplings, are discussed by Schobeiri et al.[7]

Simulation of Compressor Surge and Surge Prevention by Adjusting Stator Blades

The surge prevention capability of the presented method is demonstrated by simulating the dynamic behavior of an actual

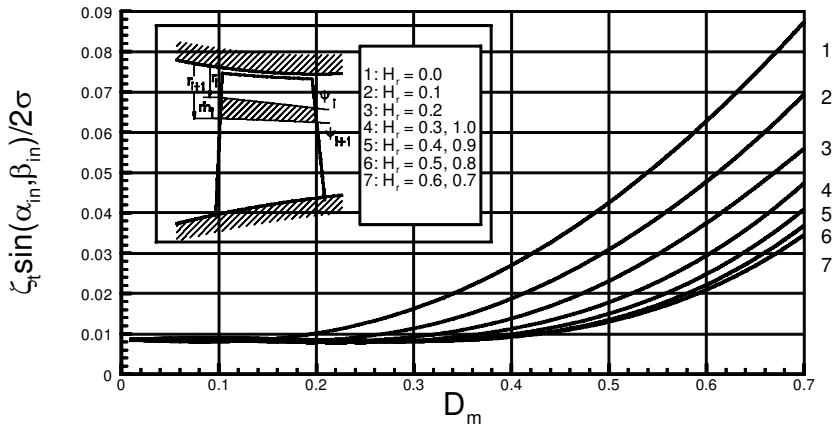

Fig. 2 Total loss parameter as a function of the modified diffusion factor D_m with immersion factor as parameter, from Schobeiri.[4]

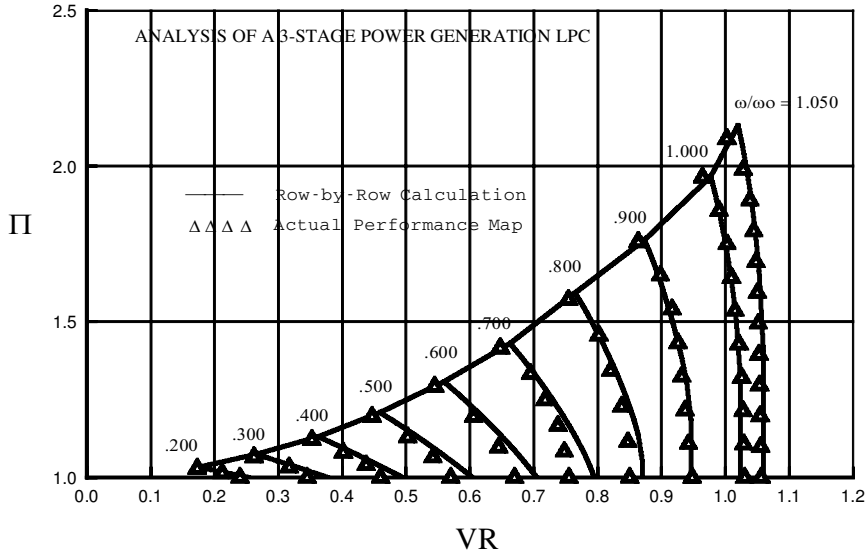

Fig. 3 Row-by-row reproduced performance map of the three-stage LP compressor for the gas turbine GT9: △, actual performance map.

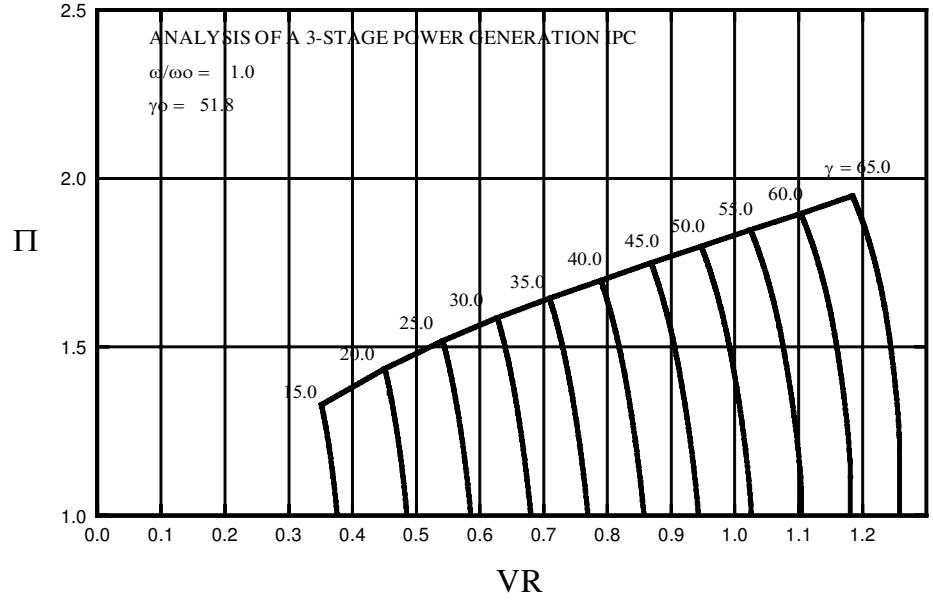

Fig. 4 Row-by-row generated performance map with stator stagger angle as parameter for the IP compressor.

single-spool gas turbine engine with a power shaft split under an adverse transient operation condition, as shown in Fig. 5. The gas generator unit incorporates a multistage compressor that we decompose into LP, IP, and HP compressor, as discussed earlier. The compressor is followed by a combustion chamber, a three-stage turbine that drives the compressor, and a two-stage power turbine connected with a generator. The LP–IP–HP compressor is modeled using the row-by-row method presented in this Note. The simulation schematic of the engine is shown in Fig. 6, where the individual components are placed between the plena. Figure 6 also shows the interaction of individual components with the control system. As seen in Fig. 6, the speed controller is connected to the power shaft, which senses the rotational speed and the turbine inlet temperature of the power shaft and its time derivative to control the fuel mass flow.

Case 1: Simulation of Compressor Surge

When started from a steady-state operating point, the dynamic behavior of the described engine is simulated for a transient operation, which is controlled by the prescribed load schedule that acts on the power shaft as shown in Fig. 7. Following this schedule, we first simulate an abrupt loss of load, which represents a sudden partial generator trip. Because of the sudden loss of load, the power-generation shaft reacts to this event with a corresponding increase in rotational speed (Fig. 8). This increase in rotational speed causes the controller to trigger a rapid throttling of the fuel mass flow. The throttling process lasts until a constant idling speed of the power shaft is attained. After about 7 s, full load is suddenly added and then reduced slowly such that, after the completion of the load addition, the gas turbine is supplying 25% of its rated load (Fig. 7). The rotor reacts to this sudden addition of load with a sharp decrease in rotational speed. That, in turn, causes a quick opening of the fuel valve. During this process, the power-generation capability of the gas-generation turbine deteriorates significantly, causing a major power imbalance between the turbine and compressor components (Fig. 8). This imbalance results in a continuous decrease of the compressor rotor speed, causing the compressor to operate partially in rotating stall and surge regimes. As shown in Fig. 9, reducing the rotor speed below 90% forces the LP-compressor stage group into rotating stall and a short-duration surge process with a reversal

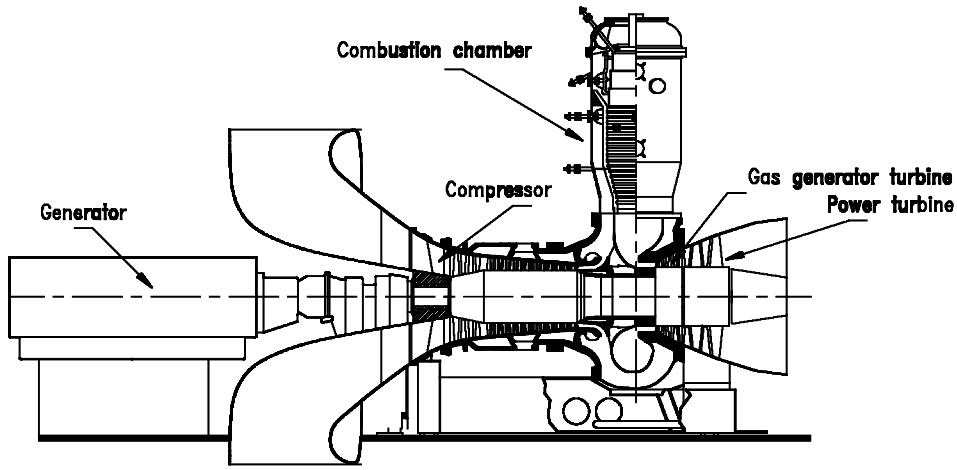

Fig. 5 Single-spool split shaft power-generation gas turbine engine, derivative from GT-9.

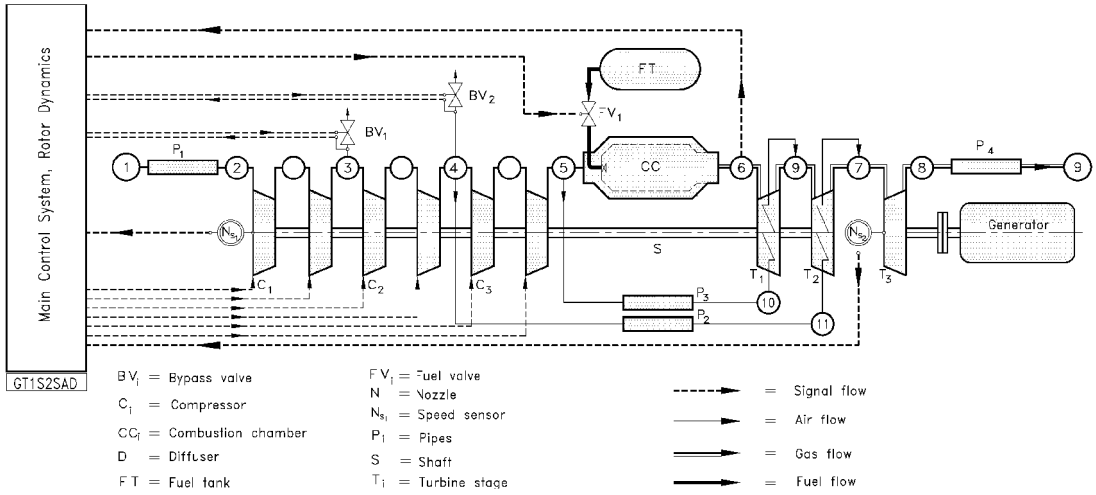

Fig. 6 Simulation schematic of gas turbine engine shown in Fig. 5.

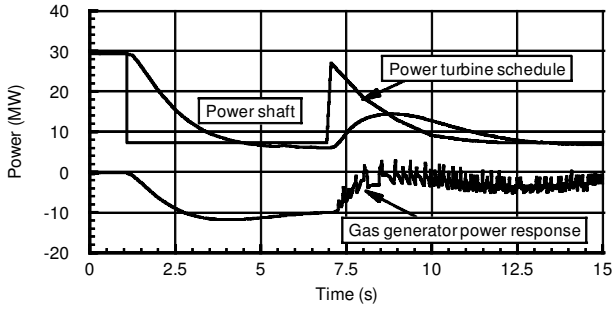

Fig. 7 Power turbine load schedule by the generator.

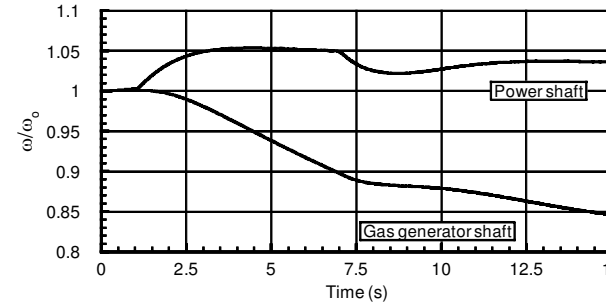

Fig. 8 Rotational speed of power shaft and gas generator.

in the mass flow direction. Because the magnitude of the reversed mass flow is relatively small and of very short duration, a total engine mass flow reversal does not occur. The IP-compressor stage group exhibits similar instability behavior, where the compressor mass flow reversal occurs at slightly lower frequency and almost the same amplitude. The HP-stage group displays a distinctively different behavior. Whereas the mass flow experiences a fluctuation at a similar frequency, the amplitude remains always positive. These fluctuations apparently are not caused by the HP-stage group itself, but are propagated downstream from LP and IP parts, respectively. This behavior is fully consistent with the continuity requirement that leads to an integrally positive mass flow rate because of the high-frequency and short-duration mass flow reversal in LP and IP compressors.

Case 2: Instability and Surge Prevention by Stator Stagger Angle Adjustment

To prevent the compressor instability and surge described in case 1, the stagger angles of the LP- and IP-compressor stage groups were dynamically adjusted. Similar to case 1, the engine was forced into an adverse off-design operation condition with the same load schedule as shown in Fig. 7. When started from the steady-state point, in accordance with the load schedule shown in Fig. 10, first a generator loss of load was simulated. The power-generation shaft responds to this event with a rapid increase in rotational speed, which triggers closing of the fuel valve. As a consequence, without active control, the power of the gas-generation turbine would not be sufficient to cover the power consumption of the compressor. As observed in case 1, this imbalance of power has led to a decrease in

rotational speed of the gas-generation shaft, which forced the first two compressor stage groups into an unstable regime.

To avoid the power imbalance of the gas-generation shaft as in case 1, the stagger angle pertaining to the stator blades of the LP- and IP-stage groups are continuously reduced according to the prescribed schedule. This procedure starts immediately at the time where the loss of load occurs and lasts until the prescribed γ values at $t = 4$ s are reached. These values are kept constant for the rest of the simulation.

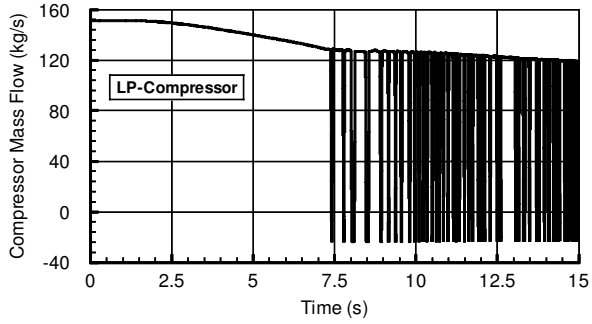

Fig. 9 LP-compressor mass flow as function of time; instability starts after sudden load addition was completed; stator blades are not adjusted.

As shown, it is sufficient to reduce the stagger angle of the LP and IP compressors, while the stagger angle of the HP compressor remained unchanged. This intervention causes a substantial shift in the surge limit preventing all three compressor stage groups from entering into the instability regime. The compressor mass flow does not experience any fluctuations. The stable operation of the compressors is reflected in Fig. 10, where the load schedule and the response of power-generator and gas-generator turbines are shown. In contrast to the unadjusted case 1 shown in Fig. 7, no power fluctuations are encountered.

The rotational speed behavior of the gas-generator shaft shown in Fig. 11 is substantially different from the one shown in case 1. The positive power difference prevents the rotational speed from decreasing, which, associated with lower pressure ratio, moves the compressor operation to a more stable operation regime. The power generator shaft, however, behaves very similar to case 1.

Conclusions

A method of active aerodynamic control and prevention of axial compressor instability and surge was presented that was based on dynamically adjusting the compressor stator blades during adverse operation. To demonstrate the capability of the method, it was applied to a single-spool, two-shaft power-generation gas turbine engine with a multistage compressor. Two complete dynamic engine simulations were performed. In the course of the first simulation, the stator-row stagger angles were kept at their design point, and the compressor was forced into an unstable operation mode. As a

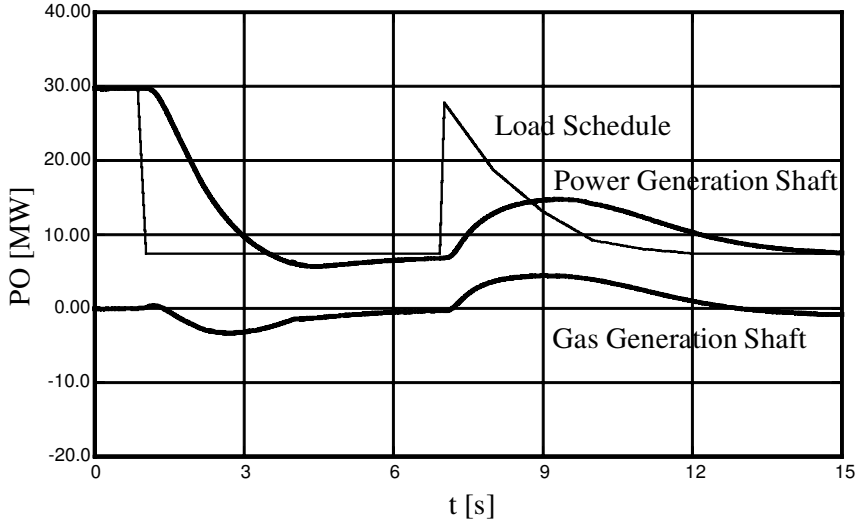

Fig. 10 Power response of gas generator and power turbine shaft following a dynamic stator stagger angle adjustment.

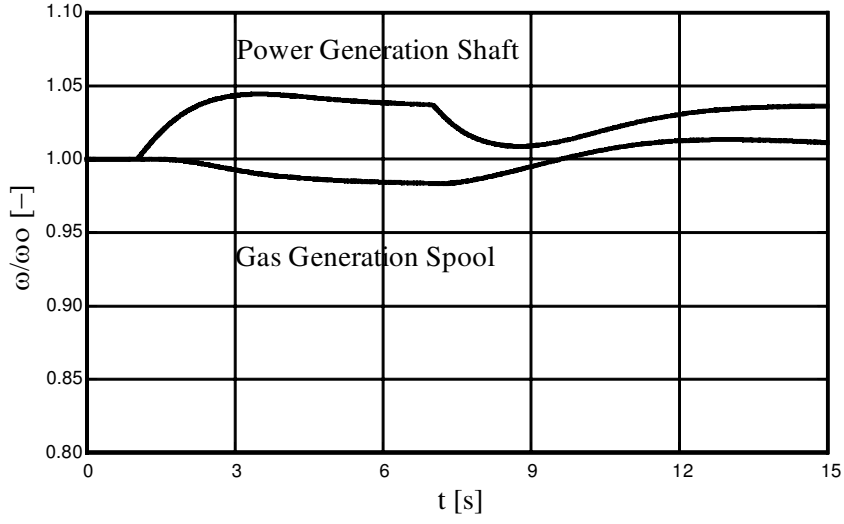

Fig. 11 Rotational speed of gas generator and power turbine shaft following a dynamic adjustment of stator stagger angle.

result, both the LP- and the IP-compressor stage groups revealed high-frequency, short-duration mass flow fluctuations with large amplitudes and alternatively positive and negative values. The HP-compressor stage group exhibited only positive mass flow fluctuations. These fluctuations were apparently propagated downstream and did not originate from the HP part. Introducing the stator blade stagger angle adjustment brought substantial change in operational behavior. Adjusting the LP- and IP-compressor stagger angle caused a significant shift in surge limit and established a fully stable operation regime for all three compressor parts.

References

[1]Schlichting, H., "Die Grenzschicht mit Absaugung und Ausblasen," Luftfahrtforschung, No. 19, 1942, pp. 239–301.

[2]Betz, A., "History of Boundary Layer Control in Germany," *Boundary Layer and Flow Control*, Vol. 1, 1961, pp. 1–20.

[3]Greitzer, E. M., "Stability of Pumping Systems," *Journal of Fluids Engineering*, Vol. 103, June 1981, pp. 193–238.

[4]Schobeiri, M. T., "New Shock Loss Model for Transonic and Supersonic Axial Compressors with Curved Blades," *Journal of Propulsion and Power*, Vol. 14, No. 4, 1998, pp. 470–478.

[5]Schobeiri, M. T., "Active Aerodynamic Control of Multi-stage Axial Compressor Instability and Surge by Dynamically Adjusting the Stator Blades," American Society of Mechanical Engineers, ASME-Paper GT-0479, June 2001.

[6]Attia, M. S., and Schobeiri, M. T., "A New Method for the Prediction of Compressor Performance Maps Using One-Dimensional Row-by-Row Analysis," American Society of Mechanical Engineers, ASME-Paper 95-GT-434, June 1995.

[7]Schobeiri, M. T., Abouelkheir, M., and Lippke, C., "GETRAN: A Generic, Modularly Structured Computer Code for Simulation of Dynamic Behavior of Aero- and Power Generation Gas Turbine Engines," *Journal of Gas Turbine and Power*, Vol. 1, July 1994, pp. 483–494.

Aerodynamic Design of a Vertical-Thrust Adapter for Jet Engines

T. Strand*
San Diego, California 92107

Introduction

SUPPOSE we want to change the direction of the thrust of the jet engines of a hypothetical stationary multiengined vertical takeoff and landing (VTOL) aircraft from horizontal to vertical. One approach might be to tilt each engine 90 deg. Another might be to tilt the exhaust nozzles only. A third and possibly simpler approach might be, if feasible, to guide the horizontal flow, issuing from each nozzle, through a right angle turn by having it follow along a two-dimensional curved barrier. This latter, novel concept is the subject of the present aerodynamic design study.

To obtain two-dimensional flow, we shall assume that the cross section of the exhaust nozzle, instead of being circular, is square, and that the jet is constrained to flow along a curved barrier between two vertical walls (endplates) attached to the sides of the barrier. The flow model assumed and the coordinate system used are shown in Fig. 1a.

The barrier blocks the horizontal flow and turns the flow downward through a right angle. We shall assume the barrier to consist of a curved constant-velocity (streamline) section, conjoined to two straight sections, one of which is attached to the nozzle. The straight sections serve to guide the decelerating flow to—and the accelerating flow from—the curved section. Two free streamlines, extending to infinity downstream, complete the description of the thrust adapter.

Hence, we shall be dealing with a two-dimensional gas flow in which the bounding walls are either straight or have constant velocity. Textbooks on compressible fluid flow (see for instance Refs. 1–4) show that the solution to this type of configuration can be obtained by modifying the solution to its incompressible flow counterpart, provided the Chaplygin–Karman–Tsien tangent-gas approximation is substituted for the isentropic relations. In the counterpart (related) flow the lengths of—and the velocity magnitudes along—the boundaries are different from those in the compressible flow, but the velocity inclination angles are identical at corresponding points. We shall, therefore, first obtain the solution to the incompressible flow problem. Next, this solution will be modified for compressibility.

No new theories or methods will be introduced. Textbook aerodynamic theory will be employed to calculate the shape of a sample unique barrier and the pressure coefficients along the boundaries.

Several authors have studied other two-dimensional configurations having boundaries consisting of combinations of straight lines and free streamlines. Some of these are discussed in Ref. 4.

Incompressible Flow Solution

The problem will be formulated as a boundary-value problem and will be solved through use of a conformal mapping scheme. Consider then the incompressible flow within the boundaries ABB′CDEA′ in Fig. 1a. One flow property must be specified along each boundary.

The pressure is constant along the two free streamlines AB and EA′. The velocity magnitude q therefore has some constant value here, say U_0. Across the nozzle exhaust BB′ and along the straight section B′C, the inclination angle θ of the velocity vector is zero. Along the curved section C D, the velocity magnitude will be assumed constant, say U_1. The angle of the straight section DE will also be assumed given, say θ_1. Note that this angle is negative in the chosen coordinate system. We shall also specify a point value U_2 of the velocity magnitude at B′. Thus, after nondimensionalizing the given velocity magnitudes, we end up with three input parameters for the related incompressible flow, namely, U_1/U_0, U_2/U_0, and θ_1.

As just mentioned, the jet issues normal to the nozzle exhaust plane. Therefore, the velocity potential φ is constant along this

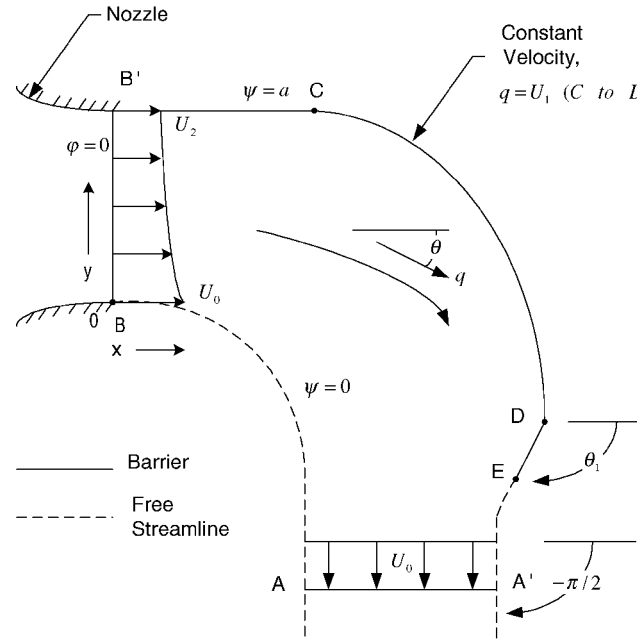

Fig. 1 Adapter, side view—flow model and coordinate system; and shape (to scale) of barrier and free streamlines for $M_0 = 0.95$, $U_1^*/U_0^* = 0.25$, $U_2^*/U_0^* = 0.92$, and $\theta_1 = -105$ deg.

Received 19 November 2001; revision received 30 October 2002; accepted for publication 8 November 2002.

*Former Member AIAA, Aeronautical Engineer, retired.